J. Fluid Mech. (1976), *vol.* 77, *part* 4, *pp.* 625–644
Printed in Great Britain

Separation from the surface of two equal spheres in Stokes flow

By A. M. J. DAVIS, M. E. O'NEILL

Department of Mathematics, University College London, Gower Street, London WC1E 6BT, England

J. M. DORREPAAL

Department of Mathematics, University of British Columbia, Vancouver, Canada V6T 1W5†

AND K. B. RANGER

Department of Mathematics, University of Toronto, Toronto, Canada M5S 1A1

(Received 1 May 1976)

In this paper, it is shown that if two spheres of equal radii are placed axisymmetrically in a steady Stokes stream, separation of the flow from the spheres occurs if the distance between their centres is less than approximately 3·57 times the sphere radius. For spheres whose spacing is less than this value, wakes form on both spheres and the fluid within the wakes moves in closed eddy type motion. When the distance between the centres of the spheres is less than approximately 3·22 times the sphere radius, a cylinder of fluid links both spheres, and within this cylinder the fluid rotates in one or more ring vortices, the number of vortices increasing as the distance between the spheres is decreased. When the spheres are in contact, the fluid rotates in an infinite set of nested ring vortices.

1. Introduction

The possibility of separation of a flow from a boundary is a relatively recent development in the study of Stokes flows. Jeffery (1922) seems to be the first author to have produced a solution to a Stokes flow problem which exhibits this phenomenon. He considered the flow generated between two parallel eccentric circular cylinders which rotate about their axes, and from his solution, which was expressed in bipolar co-ordinates, Jeffery determined the drag and torque coefficients for the cylinders. However he did not show that the flow separates for sufficiently large eccentricity. This was demonstrated by Wannier (1950), who, apparently unaware of Jeffery's work derived the solution of the problem in a different form. Wannier showed that, if the outer cylinder is at rest and the inner cylinder rotates with constant angular velocity, then, for sufficiently large eccentricity, a branch of the stream surface $\psi = 0$ divides the flow into two

† Present address: Department of Mathematical and Computing Science, Old Dominion University, Norfolk, Virginia, 23508, U.S.A.

parts. One part of the flow rotates about, and in the same sense as, the rotating cylinder, while, in the other part of the flow, the fluid rotates in the opposite sense to the rotating cylinder in a closed region adjacent to the outer fixed cylinder.

It is also possible to show from Jeffery's solution that for the case of two cylinders of equal radius external to each other, and rotating with angular velocities of equal magnitude but of opposite sense in an infinite fluid, a uniform stream is induced at infinity which is directed normal to the plane containing the axes of the cylinders. From Jeffery's expression for the stream function, it can be shown that the cylinders are enclosed by the stream surface $\psi = 0$, which separates the fluid which flows past the cylinders from that which is trapped in a closed circulatory motion about the cylinders.

A more recent and different example of a separating Stokes flow is that described in papers by Dean & Montagnon (1949) and Moffatt (1964) for the two-dimensional motion interior to a wedge-shaped region. By considering solutions of the plane biharmonic equation in polar co-ordinates, Dean & Montagnon showed that the power of the radial co-ordinate in the solution is complex if the angle of the wedge is less than about 146°, which was interpreted by Moffatt as indicating the existence of an infinite sequence of eddies near the corner. Schubert (1967) showed that the same phenomenon occurs in the neighbourhood of the cusp when there is a shear flow over a circular cylinder in contact with a plane. Wakiya (1975) has considered the more general case when the cylinder intersects the plane, and shows that an infinite sequence of eddies occurs in the neighbourhood of the intersection line if the angle of intersection between the cylinder and the plane is less than the critical Dean–Moffatt angle. A three-dimensional analogue of these results is the infinite set of ring vortices which Dorrepaal *et al.* (1976*a*) have shown to exist in the conical cusps of a closed torus when placed axisymmetrically in a uniform stream. A similar result has been derived numerically by Bourot (1975) for the case of a cardioid of revolution. A further example of a three-dimensional Stokes flow which separates is the axisymmetric flow past a spherical cap. Dorrepaal, O'Neill & Ranger (1976*b*) have demonstrated that separation occurs at the rim of the cap for all non-zero angles subtended at the centre of the sphere of the cap. When this angle tends to zero and the cap degenerates into a circular disk, the flow does not separate.

In the foregoing examples, the flows are either two-dimensional or involve a three-dimensional body with a re-entrant boundary. The present paper is concerned with convex bodies, namely two equal spheres which are fixed axisymmetrically in a uniform stream of infinite viscous fluid. The exact solution for the Stokes flow past these bodies was obtained by Stimson & Jeffery (1926), when the spheres are not in contact, and by Cooley & O'Neill (1969) when the spheres are in contact. These authors provided expressions for the forces acting on the spheres but did not discuss the structure of the flows, which was the motivation of the investigation reported in this paper. It is well known that, for a sphere in isolation in a uniform stream, no separation of the flow from the body occurs. This is found to be true for the case of two spheres when the distance between the centres of the spheres is greater than approximately 3·57 times the

sphere radius. For spheres whose spacing is less than this value, there is fluid attached to either sphere which moves in closed eddy type motion, in wakes attached to each sphere if the spacing between the centres of the spheres exceeds about 3·22 times the radius. At this spacing, the wakes coalesce and, for smaller spacings, there is a cylinder of fluid attached to both spheres such that the fluid rotates in one or more ring vortices, the number increasing as the spheres come closer together. In the case of contact between the spheres, the fluid within the cylinder rotates in an infinite set of nested ring vortices.

2. Statement of the problem

Two rigid spheres, each of radius a, are placed in a steady stream of infinite incompressible viscous fluid of constant density ρ and viscosity μ, so that the line of centres of the spheres, which are held at rest, is parallel to the direction of the stream. The speed of the stream is U and the distance between the centres of the spheres is $2ka$ with $k > 1$, as illustrated in figure 1.

Choose cylindrical polar co-ordinates (ar, θ, az), so that the centres of the spheres are at $r = 0$, $z = \pm k$. Then, because the flow is symmetrical about the z axis, it follows that the fluid velocity has cylindrical components of the form $U(u, 0, w)$, with u and w independent of θ. Assuming that the Reynolds number $Ua\rho/\mu$ for the flow is sufficiently small to allow the inertia terms in the Navier–Stokes equations to be neglected, it follows that the equations governing the motion of the fluid are

$$\nabla p = \mu \nabla^2 \mathbf{v}, \quad \nabla . \mathbf{v} = 0, \tag{2.1}$$

where p is the hydrodynamic fluid pressure. The second of these equations implies the existence of a Stokes stream function ψ which is defined by

$$u = \frac{1}{r}\frac{\partial \psi}{\partial z}, \quad w = -\frac{1}{r}\frac{\partial \psi}{\partial r}. \tag{2.2}$$

The elimination of p from the first of equations (2.1) shows that ψ satisfies the equation

$$\Lambda^4 \psi = \left(\frac{\partial^2}{\partial r^2} - \frac{1}{r}\frac{\partial}{\partial r} + \frac{\partial^2}{\partial z^2}\right)^2 \psi = 0. \tag{2.3}$$

The boundary conditions require that $u = w = 0$ on either sphere and, if the undisturbed stream is along the negative z direction, then $u = 0$, $w = -1$ at infinity. These boundary conditions will be satisfied if, on either sphere,

$$\psi = \frac{\partial \psi}{\partial n} = 0, \tag{2.4}$$

where $\partial/\partial n$ denotes the derivative along the outward normal to either sphere, and

$$\psi \sim \tfrac{1}{2} r^2 \tag{2.5}$$

as $r^2 + z^2 \to \infty$.

The boundary-value problem posed by equations (2.3), (2.4) and (2.5) possesses a unique solution, as shown, for instance, by Finn & Noll (1957). We shall consider in turn the properties of this solution for the cases of spheres in contact ($k = 1$) and separated spheres ($k > 1$).

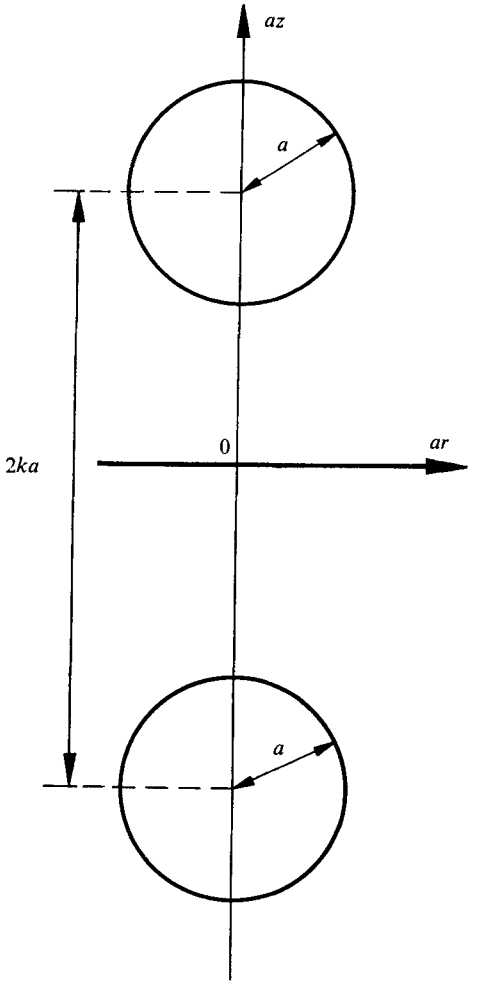

FIGURE 1. The geometry of the problem.

3. Spheres in contact

The solution for the stream function is most conveniently represented by means of tangent-sphere co-ordinates (ξ, θ, η) defined by

$$r = \frac{2\eta}{\xi^2+\eta^2}, \quad z = \frac{2\xi}{\xi^2+\eta^2}. \tag{3.1}$$

The spheres are given by $\xi = \pm 1$ and the flow region by $|\xi| < 1$, $0 \leqslant \eta < \infty$, $0 \leqslant \theta \leqslant 2\pi$. The boundary conditions (2.4) and (2.5) are equivalent to

$$\psi = \frac{\partial \psi}{\partial \xi} = 0 \quad (\xi = \pm 1), \tag{3.2}$$

$$\psi - \frac{2\eta^2}{(\xi^2+\eta^2)^2} \to 0 \quad \text{as} \quad (\xi^2+\eta^2) \to 0. \tag{3.3}$$

The solution for ψ may be written down by adding $2\eta^2(\xi^2+\eta^2)^{-2}$ to the solution found by Cooley & O'Neill (1969) for the problem when the spheres translate along their line of centres through a quiescent fluid. Consequently,

$$\psi = \frac{\eta}{(\xi^2+\eta^2)^{\frac{3}{2}}}\int_0^\infty (B\cosh s\xi + \xi C\sinh s\xi)\,J_1(s\eta)\,ds + \frac{2\eta^2}{(\xi^2+\eta^2)^2}, \tag{3.4}$$

where

$$B = -\frac{2+2s+s^{-1}(1-e^{-2s})}{s+\sinh s\cosh s}, \quad C = \frac{1+2s-e^{-2s}}{s+\sinh s\cosh s}.$$

It is clear that $\psi(-\xi,\eta) = \psi(\xi,\eta)$, and by means of the Hankel transform

$$\eta(\xi^2+\eta^2)^{-\frac{1}{2}} = \int_0^\infty e^{-s|\xi|}(|\xi|+s^{-1})\,J_1(s\eta)\,ds,$$

it follows that, for $0 \leqslant \xi \leqslant 1$,

$$\psi = -\frac{2\eta}{(\xi^2+\eta^2)^{\frac{3}{2}}}\frac{d}{d\eta}\int_0^\infty \frac{J_0(s\eta)}{2s+\sinh 2s}\,f(\xi,s)\,ds, \tag{3.5}$$

where

$$\begin{aligned} f(\xi,s) = {} & \xi\{s^{-1}\sinh s\xi + 2\cosh s\xi + s^{-1}\sinh(2-\xi)\,s\} \\ & - 2s^{-1}\sinh s\xi - 2\cosh s\xi - s^{-2}\cosh s\xi + s^{-2}\cosh(2-\xi)\,s. \end{aligned} \tag{3.6}$$

It may be easily verified that $f(\xi, s)$ is an even function of s which vanishes at $s = 0$. Furthermore $f(\xi, s)$ is regular in the complex s plane and is real valued whenever s^2 is real.

The integral representation

$$J_0(x) = \frac{2}{\pi}\int_1^\infty \frac{\sin tx}{(t^2-1)^{\frac{1}{2}}}\,dt \quad (x > 0),$$

given in Abramovitz & Stegun (1965), enables (3.5) to be rewritten as

$$\psi = \frac{2\eta i}{\pi(\xi^2+\eta^2)^{\frac{3}{2}}}\frac{d}{d\eta}\int_1^\infty \frac{dt}{(t^2-1)^{\frac{1}{2}}}\int_{-\infty}^\infty \frac{f(\xi,s)\,e^{is\eta t}}{2s+\sinh 2s}\,ds. \tag{3.7}$$

With $f(\xi, s)$ given by (3.6) and $0 \leqslant \xi \leqslant 1$, the s-integral can be expressed as a sum of residues at the zeros of $2s+\sinh 2s = 0$ in the upper half of the complex s plane.

The zeros of $z+\sin z = 0$ are $z = \pm\lambda_n$ and $z = \pm\bar{\lambda}_n$ $(n = 1, 2,\ldots)$, where each λ_n is in the first quadrant, $\bar{\lambda}_n$ is the complex conjugate of λ_n, and the ordering is according to increasing real part. Buchwald (1964) has tabulated the first few values of λ_n, namely

$$\left.\begin{aligned} \lambda_1 &= 4{\cdot}21239 + 2{\cdot}25073i, \\ \lambda_2 &= 10{\cdot}7125 + 3{\cdot}10319i, \\ \lambda_3 &= 17{\cdot}0734 + 3{\cdot}55108i, \end{aligned}\right\} \tag{3.8}$$

to six significant figures. As $n \to \infty$, λ_n can be calculated from the asymptotic expansion:

$$\lambda_n \sim \alpha_n - \alpha_n^{-1}\log(2\alpha_n) + i\log(2\alpha_n),$$

where $\alpha_n = (2n-\frac{1}{2})\pi$, which is useful in starting a Newton iteration procedure for determining λ_n numerically.

The zeros of $2s+\sinh 2s = 0$ in the upper half of the complex s-plane are evidently $s = \frac{1}{2}i\lambda_n$ and $s = \frac{1}{2}i\bar{\lambda}_n$ $(n = 1, 2, \ldots)$. Hence (3.7) may be written as

$$(\xi^2+\eta^2)^{\frac{3}{2}}\psi/2\eta = -\mathrm{Re}\frac{d}{d\eta}\int_1^\infty \frac{2\,dt}{(t^2-1)^{\frac{1}{2}}}\sum_{n=1}^{\infty}\frac{f(\xi, \frac{1}{2}i\lambda_n)}{1+\cos\lambda_n}e^{-\frac{1}{2}\lambda_n\eta t}.$$

It is of particular interest to know the behaviour of ψ in the neighbourhood of the point of contact between the spheres. Here $\eta > 2$, so, with exponentially small error, only the first term in the series need be retained, giving

$$\begin{aligned}(\xi^2+\eta^2)^{\frac{3}{2}}\psi/2\eta &\sim -\mathrm{Re}\frac{2f(\xi, \frac{1}{2}i\lambda_1)}{1+\cos\lambda_1}\frac{d}{d\eta}\int_1^\infty \frac{e^{-\frac{1}{2}\lambda_1\eta t}}{(t^2-1)^{\frac{1}{2}}}dt \\ &= \mathrm{Re}\frac{\lambda_1 f(\xi, \frac{1}{2}i\lambda_1)}{1+\cos\lambda_1}K_1(\tfrac{1}{2}\lambda_1\eta) \\ &\sim \mathrm{Re}\frac{\lambda_1 f(\xi, \frac{1}{2}i\lambda_1)}{1+\cos\lambda_1}\left(\frac{\pi}{\lambda_1\eta}\right)^{\frac{1}{2}}e^{-\frac{1}{2}\lambda_1\eta}\left[1+\frac{3}{4\lambda_1\eta}+O(\lambda_1^{-2}\eta^{-2})\right].\end{aligned}$$

Since λ_1 is complex, the exponential function of η is oscillatory with period $4\pi/\mathrm{Im}(\lambda_1)$. Hence, for all ξ in the range $0 \leqslant \xi < 1$, there is an infinity of values of η for which ψ vanishes. Since the flow is symmetrical about the plane $z = 0$ and the axis $r = 0$, it follows that there exists an infinite set of stream surfaces of revolution on which $\psi = 0$. These surfaces bound an infinite set of nested ring vortices with axes along the z axis, and are attached to the spheres where

$$\chi(\eta) = \lim_{\xi\to 1}\left\{\frac{\psi(\xi,\eta)}{(1-\xi)^2}\right\} = \lim_{\xi\to -1}\left\{\frac{\psi(\xi,\eta)}{(1+\xi)^2}\right\} = 0. \tag{3.9}$$

From (3.6),

$$\lim_{\xi\to 1}\frac{f(\xi, \frac{1}{2}i\lambda_1)}{(1-\xi)^2} = -\lambda_1\sin\tfrac{1}{2}\lambda_1.$$

Consequently $\chi(\eta)$ is given asymptotically by

$$\frac{(1+\eta^2)^{\frac{3}{2}}\chi(\eta)}{2\eta} \sim -\mathrm{Re}\frac{\lambda_1^2\sin\frac{1}{2}\lambda_1}{1+\cos\lambda_1}\left(\frac{\pi}{\lambda_1\eta}\right)^{\frac{1}{2}}e^{-\frac{1}{2}\lambda_1\eta}\left[1+\frac{3}{4\lambda_1\eta}+O(\lambda_1^{-2}\eta^{-2})\right]$$

when $\eta \gg 2$. Thus the solutions of (3.9) are given asymptotically by

$$\begin{aligned}\tfrac{3}{2}\arg(\lambda_1)+\arg(\sin\tfrac{1}{2}\lambda_1)-\arg(1+\cos\lambda_1) \\ -\tfrac{1}{2}\eta\,\mathrm{Im}(\lambda_1)+\arg(1+3/4\lambda_1\eta) \sim -(m+\tfrac{1}{2})\pi,\end{aligned} \tag{3.10}$$

with $m = 0, \pm 1, \pm 2, \ldots$. When λ_1 is given by (3.8), it follows that the positive solutions of (3.10) are given asymptotically by

$$\tfrac{1}{2}\eta\,\mathrm{Im}(\lambda_1)-\arg(1+3/4\lambda_1\eta) \sim d_m, \tag{3.11}$$

where $d_1 = 3{\cdot}12411$ and $d_m - d_{m-1} = \pi$ $(m = 2, 3, \ldots)$. Since $\arg(1+3/4\lambda_1\eta) \ll 1$ when $|\lambda_1|\eta \gg 1$, the asymptotic equation (3.11) can be conveniently solved by the iterative scheme

$$\begin{aligned}\tfrac{1}{2}\eta_0\,\mathrm{Im}(\lambda_1) &= d_m, \\ \tfrac{1}{2}\eta_j\,\mathrm{Im}(\lambda_1) &= d_m+\arg(1+3/4\lambda_1\eta_{j-1}) \quad (j \geqslant 1),\end{aligned}$$

zeros of $\chi(\eta)$			zeros of $\psi(0, \eta)$		
m	η	r	η	r	w_0
1	2·755	0·6414	3·047	0·6564	$-6{\cdot}0\times10^{-4}$
2	5·562	0·3483	5·847	0·3420	$1{\cdot}2\times10^{-6}$
3	8·352	0·2361	8·642	0·2314	$-2{\cdot}6\times10^{-9}$

TABLE 1

the suffix j denoting the jth approximation. It can readily be shown that the convergence factor

$$\frac{\eta_{j+1}-\eta_j}{\eta_j-\eta_{j-1}} \sim \frac{24}{|3+4\eta\lambda_1|^2} < \frac{1}{12d_m^2}.$$

The accuracy of a solution of (3.11) as a solution of (3.9) can be improved by considering the error, which is

$$\begin{aligned}\frac{2}{\operatorname{Im}(\lambda_1)}\left[\arg(1+3/4\lambda_1\eta)-\arg\left\{1+\frac{3}{4\lambda_1\eta}-\frac{15}{32\lambda_1^2\eta^2}+O(\lambda_1^{-3}\eta^{-3})\right\}\right]&\\ \sim \frac{2}{\operatorname{Im}(\lambda_1)}\operatorname{Im}\left[\frac{15}{32\lambda_1^2\eta^2}+O(\lambda_1^{-3}\eta^{-3})\right]&\\ = -\frac{15}{8\eta^2}\frac{\operatorname{Re}(\lambda_1)}{|\lambda_1|^4}+O(\eta^{-3}).&\end{aligned}$$

Hence a positive correction is required, which, if applied, enables the values of η satisfying (3.9), and the corresponding values of $r = 2\eta(1+\eta^2)^{-1}$, to be determined correct to four significant figures. These values for the cases $m = 1, 2, 3$ are given in table 1.

The intersection of the stream surfaces $\psi = 0$ with the plane $z = 0$ can be determined by noting that (3.6) gives

$$\tfrac{1}{2}f(0, \tfrac{1}{2}i\lambda_1) = 2\lambda_1^{-2}(1-\cos\lambda_1)-1, \tag{3.12}$$

and therefore the zeros of $\psi(0, \eta)$ are given asymptotically by

$$\tfrac{1}{2}\eta\operatorname{Im}(\lambda_1)-\arg(1+3/4\lambda_1\eta) \sim e_m, \tag{3.13}$$

where $e_1 = 3{\cdot}45063$ and $e_m - e_{m-1} = \pi$ $(m = 2, 3, \ldots)$. Equation (3.13) can be solved and its solutions corrected in the same way as for the solutions of (3.11). The zeros of $\psi(0, \eta)$ and the corresponding values of $r = 2\eta^{-1}$ on the plane $z = 0$ are shown in table 1 for the three cases $m = 1, 2, 3$.

Further insight into the flow structure can be obtained by considering the velocity in the plane $z = 0$. Since ψ is an even function of ξ, the velocity component u vanishes on this plane while from (2.2) and (3.1)

$$w_0 = (w)_{z=0} = \frac{\eta^2}{4}\left(\frac{\partial\psi}{\partial\eta}\right)_{\xi=0}. \tag{3.14}$$

The zeros of w_0 occur at the centres of the sections of the ring vortices in an azimuthal plane, while the value of w_0 at a zero of $\psi(0, \eta)$ gives the maximum

velocity in the ring vortex whose outer boundary is the stream surface $\psi = 0$ through that zero. It therefore is a good measure of the decay of velocity as the point of contact between the spheres is approached.

For $\eta > 2$, we find that

$$w_0 \sim -\tfrac{1}{4}\,\mathrm{Re}\,(\lambda_1 + 5\eta^{-1} + \ldots)\frac{\lambda_1 f(0, \tfrac{1}{2}i\lambda_1)}{1+\cos\lambda_1}\left(\frac{\pi}{\lambda_1\eta}\right)^{\frac{1}{2}} e^{-\frac{1}{2}\lambda_1\eta}\left[1+\frac{3}{4\lambda_1\eta}+\ldots\right]$$

$$\sim -\tfrac{1}{4}\,\mathrm{Re}\frac{\lambda_1^2 f(0, \tfrac{1}{2}i\lambda_1)}{1+\cos\lambda_1}\left(\frac{\pi}{\lambda_1\eta}\right)^{\frac{1}{2}} e^{-\frac{1}{2}\lambda_1\eta}\left[1+\frac{23}{4\lambda_1\eta}+O(\lambda_1^{-2}\,\eta^{-2})\right],$$

where $f(0, \frac{1}{2}i\lambda_1)$ is given by (3.12). The computation of the zeros of w_0 follows in the same way as for earlier calculations. We find that the zeros corresponding to the centres of the two outermost ring vortices in the infinite nest are $\eta = 3{\cdot}38$, giving $r = 0{\cdot}592$, and $\eta = 6{\cdot}20$, giving $r = 0{\cdot}323$. At the zeros of $\psi(0, \eta)$, the velocity w_0 is the real part of $(\lambda_1 + 5\eta^{-1} + \ldots)$ times a purely imaginary expression. It is alternately positive and negative at these zeros, and

$$|w_0| \sim \tfrac{1}{4}\,\mathrm{Im}\,(\lambda_1)\left(\frac{\pi}{\eta}\right)^{\frac{1}{2}}\left[\frac{\lambda_1^{\frac{1}{2}} f(0, \tfrac{1}{2}i\lambda_1)}{1+\cos\lambda_1}\right]\left[1+\frac{3}{4\lambda_1\eta}\right] e^{-\frac{1}{2}\eta\,\mathrm{Re}\,(\lambda_1)}. \tag{3.15}$$

On substituting the computed values of η for which $\psi(0, \eta) = 0$, given in table 1, we obtain the values of w_0 displayed in the table.

Lastly, we consider the angle at which a surface of separation $\psi = 0$ detaches from either sphere. The Taylor expansion of ψ near $\xi = 1$, $\eta = \eta_*$ has the form

$$\psi(\xi, \eta) = \tfrac{1}{2}(1-\xi)^2\frac{\partial^2\psi}{\partial\xi^2} + \tfrac{1}{2}(1-\xi)^2(\eta-\eta_*)\frac{\partial^3\psi}{\partial\xi^2\partial\eta} - \tfrac{1}{6}(1-\xi)^3\frac{\partial^3\psi}{\partial\xi^3} + \ldots,$$

where all derivatives are evaluated at $(1, \eta_*)$. However, from (3.9),

$$\frac{\partial^2\psi(1,\eta)}{\partial\xi^2} = 2\chi(\eta), \tag{3.16}$$

and if separation occurs at $\eta = \eta_*$, then $\chi(\eta_*) = 0$ and the angle of separation with the tangent to the sphere is

$$\tan^{-1}\left(3\frac{\partial^3\psi}{\partial\xi^2\partial\eta}\Big/\frac{\partial^3\psi}{\partial\xi^3}\right)_{\xi=1,\,\eta=\eta_*}$$

Now
$$\frac{\partial^3\psi}{\partial\xi^3}(1, \eta_*) = \frac{8\eta_*}{(1+\eta_*^2)^{\frac{3}{2}}}\int_0^\infty \frac{s^3 J_1(s\eta_*)\cosh s\,ds}{2s+\sinh 2s},$$

and from (3.16)

$$\frac{\partial^3\psi(1,\eta_*)}{\partial\xi^2\partial\eta} = 2\chi'(\eta_*) = \frac{8\eta_*}{(1+\eta_*)^{\frac{3}{2}}}\int_0^\infty \frac{s^3\sinh s\,J_0(s\eta_*)\,ds}{2s+\sinh 2s},$$

where both expressions have been simplified by using the condition

$$\chi(\eta_*) = \frac{4\eta_*}{(1+\eta_*^2)^{\frac{3}{2}}}\int_0^\infty \frac{s^2\sinh s\,J_1(s\eta_*)}{2s+\sinh 2s}ds = 0. \tag{3.17}$$

Each of the integrals can be expanded asymptotically in the manner used for

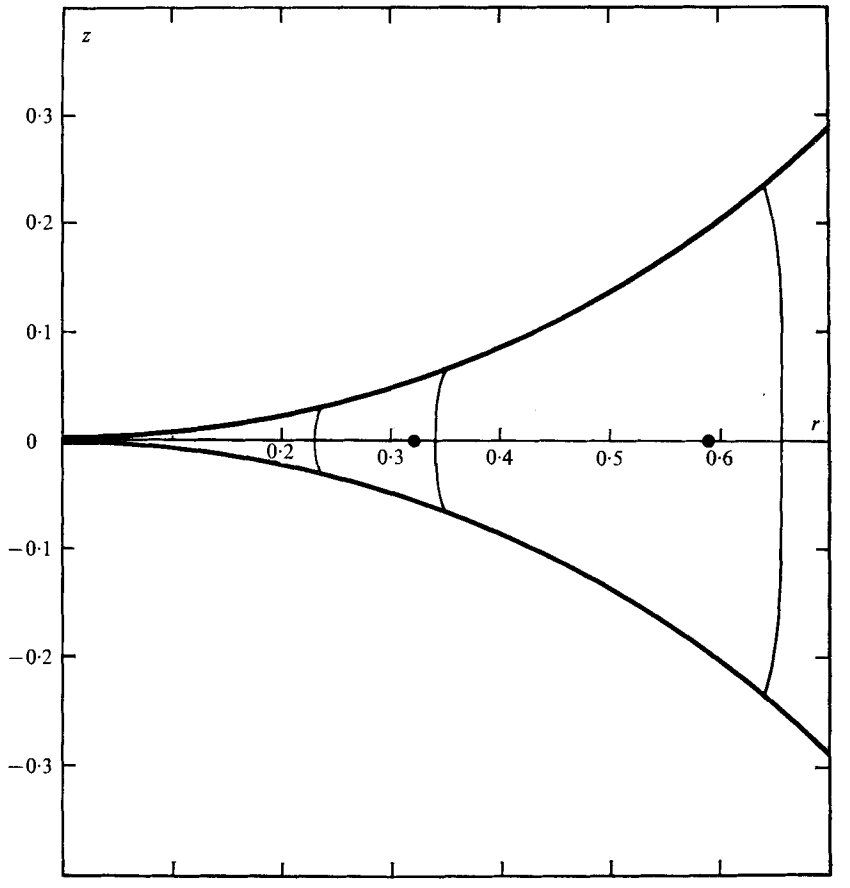

FIGURE 2. A meridional section of the separation stream surfaces. $\psi = 0$ when the spheres are in contact. The dots indicate points of zero velocity within the ring vortices.

$\chi(\eta)$ and $\psi(\xi, \eta)$ earlier in the section. By comparison with $\chi(\eta_*)$ there is a non-zero real number K such that

$$\frac{\partial^3\psi(1,\eta_*)}{\partial\xi^3} \sim -K\,\mathrm{Im}\,(\tfrac{1}{2}\lambda_1 \cot \tfrac{1}{2}\lambda_1),$$

$$\frac{\partial^3\psi(1,\eta_*)}{\partial\xi^2\partial\eta} \sim \tfrac{1}{2}K\,\mathrm{Im}\,(\lambda_1 - \eta_*^{-1} + \tfrac{3}{2}\lambda_1^{-1}\eta_*^{-2} + \ldots)$$
$$= \tfrac{1}{2}K\,\mathrm{Im}\,(\lambda_1)\{1 - \tfrac{3}{2}|\lambda_1|^{-2}\eta_*^{-2} + O(\eta_*^{-3})\}.$$

The constant K depends on η_*, but being a common factor in both expressions it is clear that to order η_*^{-1} all separation surfaces detach from the spheres at the same angle, which is 58° 36′.

Figure 2 shows the shape of the stream surfaces $\psi = 0$ when drawn using the asymptotic expressions derived in this section. It will be observed that the surfaces are essentially circular cylinders, the cross-sections tapering slightly from the circles of intersection with the spheres to the intersection with the plane $z = 0$, except for the outermost surface, where the reverse occurs, so as to preserve the near constancy of the angle of intersection of the stream surface

with either sphere. It therefore follows that, in the steady axisymmetric Stokes streaming flow past two equal spheres in contact, there is a cylinder attached to both spheres within which the fluid rotates in an infinite set of nested ring vortices. The existence of infinite sets of eddies is well known in two-dimensional Stokes flows. For instance, Dean & Montagnon (1949) and Moffatt (1964) demonstrated that such a phenomenon can occur with Stokes flows in the angle between intersecting planes provided that the angle of intersection is less than 146°. Schubert (1967) showed that the phenomenon occurs in the neighbourhood of the cusp when there is a shear flow over a circular cylinder in contact with a plane. A three-dimensional analogue of these results is the infinite set of ring vortices which Dorrepaal *et al.* (1976*a*) have shown to exist in the conical cusps of a closed torus when placed axisymmetrically in a stream. However, the phenomenon which we have demonstrated to exist in the axisymmetric streaming past two spheres in contact does not have a two-dimensional analogue. The existence of this complex flow structure when the spheres are in contact leads us to wonder how the flow structure is modified when the spheres are drawn apart. This we shall consider in the following sections.

4. Spheres not in contact

The solution for the Stokes flow produced by the translation of two equal spheres along their line of centres with the same velocity was obtained by Stimson & Jeffery (1926). Their solution for the stream function is expressed in bispherical co-ordinates defined by

$$r = \frac{c \sin \eta}{\cosh \xi - \cos \eta}, \quad z = \frac{c \sinh \xi}{\cosh \xi - \cos \eta}. \tag{4.1}$$

The spheres are given by $\xi = \pm \alpha$ ($\alpha > 0$), the radius of either sphere is c cosech α, and the distance $2k$ between the centres of the spheres is $2c \coth \alpha$. Thus, with the radii of the spheres and the distance between their centres prescribed, the quantities α and c are uniquely determined. The flow region is $-\alpha < \xi < \alpha$, $0 \leqslant \eta \leqslant \pi$, $0 \leqslant \theta \leqslant 2\pi$ and the boundary conditions (2.4) and (2.5) are now equivalent to

$$\psi = \frac{\partial \psi}{\partial \xi} = 0 \quad (\xi = \pm \alpha), \tag{4.2}$$

$$\psi - \frac{c^2 \sin^2 \eta}{2(\cosh \xi - \cos \eta)^2} \to 0 \quad \text{as} \quad \xi, \eta \to 0. \tag{4.3}$$

The solution for ψ satisfying (2.3) and the boundary conditions (4.2) and (4.3) can be obtained by adding $\frac{1}{2}c^2 \sin^2 \eta/(\cosh \xi - \cos \eta)^2$ to the solution for ψ obtained by Stimson & Jeffery. Accordingly, we have

$$\psi = c^2(\cosh \xi - \cos \eta)^{-\frac{3}{2}} \chi + \frac{c^2 \sin^2 \eta}{2(\cosh \xi - \cos \eta)^2} \tag{4.4}$$

where

$$\chi = \sum_{n=1}^{\infty} U_n V_n$$

and

$$U_n = A_n \cosh (n - \tfrac{1}{2}) \xi + C_n \cosh (n + \tfrac{3}{2}) \xi, \tag{4.5}$$

$$V_n = P_{n-1}(\cos \eta) - P_{n+1}(\cos \eta). \tag{4.6}$$

The coefficients A_n and C_n are given by

$$A_n = -\frac{n(n+1)}{\sqrt{2}(2n-1)(2n+1)} \frac{2\{1-e^{-(2n+1)\alpha}\}+(2n+1)(e^{2\alpha}-1)}{2\sinh(2n+1)\alpha+(2n+1)\sinh 2\alpha}, \tag{4.7}$$

$$C_n = \frac{n(n+1)}{\sqrt{2}(2n+1)(2n+3)} \frac{2\{1-e^{-(2n+1)\alpha}\}+(2n+1)(1-e^{-2\alpha})}{2\sinh(2n+1)\alpha+(2n+1)\sinh 2\alpha}. \tag{4.8}$$

We showed in § 3 that the flow pattern around two spheres in contact is exceedingly complex in the neighbourhood of the point of contact, there being an infinite number of circles on the spheres where the stream surfaces detach and form the boundaries of closed regions in which the fluid rotates in a system of nested ring vortices. For an isolated sphere in a uniform stream, it is well known that there is no separation of the flow from the sphere and this we expect to occur for the case of flow past two widely spaced spheres. To show that the complex flow structure for the spheres in contact develops for flow past separated spheres as the minimum clearance between the spheres approaches zero, it is most convenient to examine the behaviour of the velocity at the mid-way point between the spheres, i.e. the origin $r = z = 0$. The components $U(u_\xi, 0, u_\eta)$ of velocity in bispherical co-ordinates are

$$u_\xi = -\frac{(\cosh\xi-\sigma)^2}{c^2}\frac{\partial\psi}{\partial\sigma}, \quad u_\eta = -\frac{(\cosh\xi-\sigma)^2}{c^2(1-\sigma^2)^{\frac{1}{2}}}\frac{\partial\psi}{\partial\xi}, \tag{4.9}$$

where $\sigma = \cos\eta$. Now the origin $r = z = 0$ corresponds to $\xi = 0$, $\sigma = -1$; thus the velocity at the origin $r = z = 0$ is given by

$$u_\xi = w(0) = 1 - 4\left[\frac{\partial}{\partial\sigma}\{(\cosh\xi-\sigma)^{-\frac{3}{2}}\chi\}\right]_{\xi=0,\,\sigma=-1}, \quad u_\eta = 0. \tag{4.10}$$

It may easily be verified that, on substitution of χ from (4.5) and (4.6), equation (4.10) reduces to

$$w(0) = 1 - 4P(\alpha), \tag{4.11}$$

where

$$\begin{aligned} P(\alpha) &= (2\sqrt{2})^{-1}\sum_{n=1}^{\infty}(-1)^n(2n+1)(A_n+C_n) \\ &= \sum_{n=1}^{\infty}\frac{(-1)^{n+1}n(n+1)}{(2n-1)(2n+3)} \\ &\quad\times\frac{2(1-e^{-(2n+1)\alpha})+(2n+1)^2\sinh^2\alpha+(2n+1)\sinh 2\alpha}{2\sinh(2n+1)\alpha+(2n+1)\sinh 2\alpha}, \end{aligned} \tag{4.12}$$

on using (4.7) and (4.8). The series in (4.12) is an alternating series whose terms decrease to zero monotonically in absolute value. Thus

$$w(0) > 1 - \frac{8\{2(1-e^{-3\alpha})+9\sinh^2\alpha+3\sinh 2\alpha\}}{5(2\sinh 3\alpha+3\sinh 2\alpha)},$$

and, since the second term on the right-hand side vanishes as $\alpha\to\infty$, it follows that $w(0)$ remains positive for sufficiently large α and the direction of flow at the origin is thus the same as the stream at infinity if the spheres are sufficiently widely spaced.

To examine the behaviour of $w(0)$ as $\alpha \to 0$, we consider the function $f(z)$ defined by

$$f(z) = \frac{\pi(z^2-1)}{8(z^2-4)} \frac{2(1-e^{-\alpha z}) + z^2 \sinh^2 \alpha + z \sinh 2\alpha}{(2 \sinh \alpha z + z \sinh 2\alpha) \cos \frac{1}{2}\pi z}. \tag{4.13}$$

This function has simple poles in the complex z plane at

$$z = 2n+1 \quad (n = \pm 1, \pm 2, \ldots), \quad \pm 2 \quad \text{and} \quad \zeta_i \quad (i = 1, 2, \ldots),$$

where ζ_i are the roots of the equation

$$2 \sinh \alpha z + z \sinh 2\alpha = 0,$$

excluding $z = 0$. For all other values of z, $f(z)$ is regular.

If we consider the contour which consists of the semicircle C of radius R in the half-plane Re $(z) > 0$ with diameter Γ the line segment joining $\pm iR$, then because $\int_C f(z)\,dz \to 0$ as $R \to \infty$, it is clear that

$$\int_\Gamma f(z)\,dz = -i \int_{-\infty}^{\infty} f(iy)\,dy$$

$$= 2\pi i \text{ [sum of residues at poles of } f(z) \text{ in the half-plane Re } (z) > 0].$$

Now

$$\int_{-\infty}^{\infty} f(iy)\,dy = \frac{\pi}{4} \int_0^{\infty} \frac{y^2+1}{y^2+4} \operatorname{sech} \tfrac{1}{2}\pi y\,dy,$$

which, on using results in Gradshteyn & Ryzhik (1965), reduces to

$$\int_{-\infty}^{\infty} f(iy)\,dy = -\frac{\pi}{2} + \frac{3\pi^2}{16}. \tag{4.14}$$

The residue of $f(z)$ at $z = 2$ is $-3\pi/32$ and the sum of the residues of $f(z)$ at $z = 2n+1$ $(n = 1, 2, \ldots)$ is

$$\sum_{n=1}^{\infty} \frac{(-1)^{n+1} n(n+1)}{(2n-1)(2n+3)} \frac{2(1-e^{-(2n+1)\alpha}) + (2n+1)^2 \sinh^2 \alpha + (2n+1) \sinh 2\alpha}{2 \sinh (2n+1)\alpha + (2n+1) \sinh 2\alpha}$$

$$= P(\alpha).$$

Thus $w(0) = 1 - 4P(\alpha) = 4Q(\alpha)$, where

$$\frac{8}{\pi} Q(\alpha) = \operatorname{Re} \sum_{n=1}^{\infty} \frac{(\zeta_n^2-1)}{(\zeta_n^2-4)} \frac{2(1-e^{-\alpha\zeta_n}) + \zeta_n^2 \sinh^2 \alpha + \zeta_n \sinh 2\alpha}{(2\alpha \cosh \alpha\zeta_n + \alpha\zeta_n \sinh 2\alpha) \cos \frac{1}{2}\pi\zeta_n}. \tag{4.15}$$

When $\alpha \ll 1$, this relation gives asymptotically

$$Q(\alpha) \sim \frac{\pi}{4\alpha} \sum_{n=1}^{\infty} \frac{(a_n c_n + b_n d_n) \cos(\pi X_n/2\alpha) - (b_n c_n - a_n d_n) \sin(\pi X_n/2\alpha)}{(\cosh X_n + \cos Y_n)^2} e^{-\pi Y_n/2\alpha}, \tag{4.16}$$

where $X_n + iY_n$ $(n = 1, 2, \ldots)$ are the roots of $\sinh z + z = 0$, excluding $z = 0$, in the first quadrant, and

$$a_n = (X_n+1)^2 + 1 - Y_n^2 - 2e^{-X_n} \cos Y_n, \quad b_n = 2(X_n+1) Y_n - 2e^{-X_n} \sin Y_n,$$

$$c_n = \cosh X_n \cos Y_n + 1, \quad d_n = \sinh X_n \sin Y_n.$$

We note that $X_n + iY_n = i\bar{\lambda}_n$, with λ_n defined as in § 3. The expression (4.16) shows that the velocity of the fluid at the origin tends to zero as contact between

the spheres is approached, but that the direction of the velocity reverses infinitely many times before contact occurs. Thus the character of the flow when the spheres are close together is quite different from what it is when the spheres are widely spaced.

The velocity at any point along the line of centres between the spheres has cylindrical polar resolutes $U(0, 0, w)$, where

$$w = 1 + (\cosh\xi + 1)^2 \left[\frac{\partial}{\partial\sigma}\{(\cosh\xi - \sigma)^{-\frac{3}{2}}\chi\}\right]_{\sigma=-1},$$

which, on substitution for χ, gives

$$w = 1 + (\cosh\xi + 1)^{\frac{1}{2}} \sum_{n=1}^{\infty} (-1)^{n+1}(2n+1)\,[A_n \cosh(n-\tfrac{1}{2})\xi + C_n \cosh(n+\tfrac{3}{2})\xi], \tag{4.17}$$

with A_n and C_n given by (4.7) and (4.8). By modifying the function $f(z)$, an alternative series representation for w can be obtained which has a more suitable form than (4.17) when $\alpha \ll 1$. This series is

$$w(\xi) = \tfrac{1}{2}\pi \cosh\tfrac{1}{2}\xi \operatorname{Re} \sum_{n=1}^{\infty} (p_n \cosh\xi \cosh\tfrac{1}{2}\xi\zeta_n - q_n \sinh\xi \sinh\tfrac{1}{2}\xi\zeta_n) \tag{4.18}$$

with

$$p_n = \frac{(\zeta_n^2 - 1)}{(\zeta_n^2 - 4)} \frac{2(1 - e^{-\alpha\zeta_n}) + \zeta_n^2 \sinh^2\alpha + \zeta_n \sinh 2\alpha}{(2\alpha \cosh\alpha\zeta_n + \alpha\zeta_n \sinh 2\alpha)\cos\tfrac{1}{2}\pi\zeta_n},$$

$$q_n = \frac{(\zeta_n^2 - 1)}{(\zeta_n^2 - 4)} \frac{\zeta_n(1 - e^{-\alpha\zeta_n}) + \tfrac{1}{2}\zeta_n^2 \sinh 2\alpha + 2\zeta_n \sinh^2\alpha}{(2\alpha \cosh\alpha\zeta_n + \alpha\zeta_n \sinh 2\alpha)\cos\tfrac{1}{2}\pi\zeta_n},$$

where again the summation is taken over the zeros ζ_n of the equation

$$2\sinh\alpha z + z\sinh 2\alpha = 0$$

which are in the half-plane $\operatorname{Re}(z) > 0$.

We have calculated the values of w for $-\alpha \leqslant \xi \leqslant \alpha$, with α taking values in the range $0{\cdot}3 \leqslant \alpha \leqslant 2{\cdot}0$, using the series (4.17). Our results indicate that for all values of α greater than α_1^*, where $\alpha_1^* \approx 1{\cdot}18304$, which corresponds to a dimensionless distance $2k$ between the centres of the spheres of about 3·57, w is positive for all ξ in the range $-\alpha < \xi < \alpha$, having a maximum at $\xi = 0$ and decreasing monotonically to zero at $\xi = \pm\alpha$. If $\alpha_1^* > \alpha > \alpha_1^\dagger$, where $\alpha_1^\dagger \approx 1{\cdot}05434$, $w < 0$ for $0 \leqslant \xi_0 < |\xi| < \alpha$ and $w > 0$ for $0 \leqslant |\xi| < \xi_0$, where ξ_0 depends on α and is such that $\xi_0 = 0$ when $\alpha = \alpha_1^\dagger$. For $\alpha_1^\dagger > \alpha > \alpha_2^*$, where $\alpha_2^* \approx 0{\cdot}54587$, w is negative for all ξ in the range $0 < |\xi| < \alpha$ and monotonic increasing for $\alpha_{m_1} \geqslant \alpha > \alpha_2^*$, where $\alpha_{m_1} \approx 1{\cdot}02$. As α passes below α_2^*, zeros $\pm\xi_0$ again occur in w, with $w > 0$ for $0 \leqslant \xi_0 < |\xi| < \alpha$ and $w < 0$ for $0 < |\xi| < \xi_0$ and $\xi_0 = 0$ when $\alpha = \alpha_2^\dagger \approx 0{\cdot}51812$. As α passes below $\alpha_2^\dagger$, w becomes positive in the range $0 < |\xi| < \alpha$, the maximum in w occurring at $\xi = 0$ next when $\alpha = \alpha_{m_2} \approx 0{\cdot}508$. These changes in the profile of w in the range $0 < \xi < \alpha$ are sketched in figure 3. The cycle in the behaviour of w is then repeated as the value of α is decreased. In fact, the behaviour is repeated an infinite number of times, corresponding to the infinite number of zeros and changes in sign of $w(0)$ as $\alpha \to 0$. In table 2 we list the first five zeros of $w(0, \alpha)$ in decreasing order of magnitude.

The table shows that the zeros become closely packed as the spheres approach

$\alpha^{\dagger}$	$2k$	ϕ_c
1·05434	3·2185	31·94°
0·51812	2·2745	34·85
0·3497	2·124	35·41
0·2652	2·071	35·61
0·2140	2·046	35·71

TABLE 2. Values of the first five zeros of $w(0)$

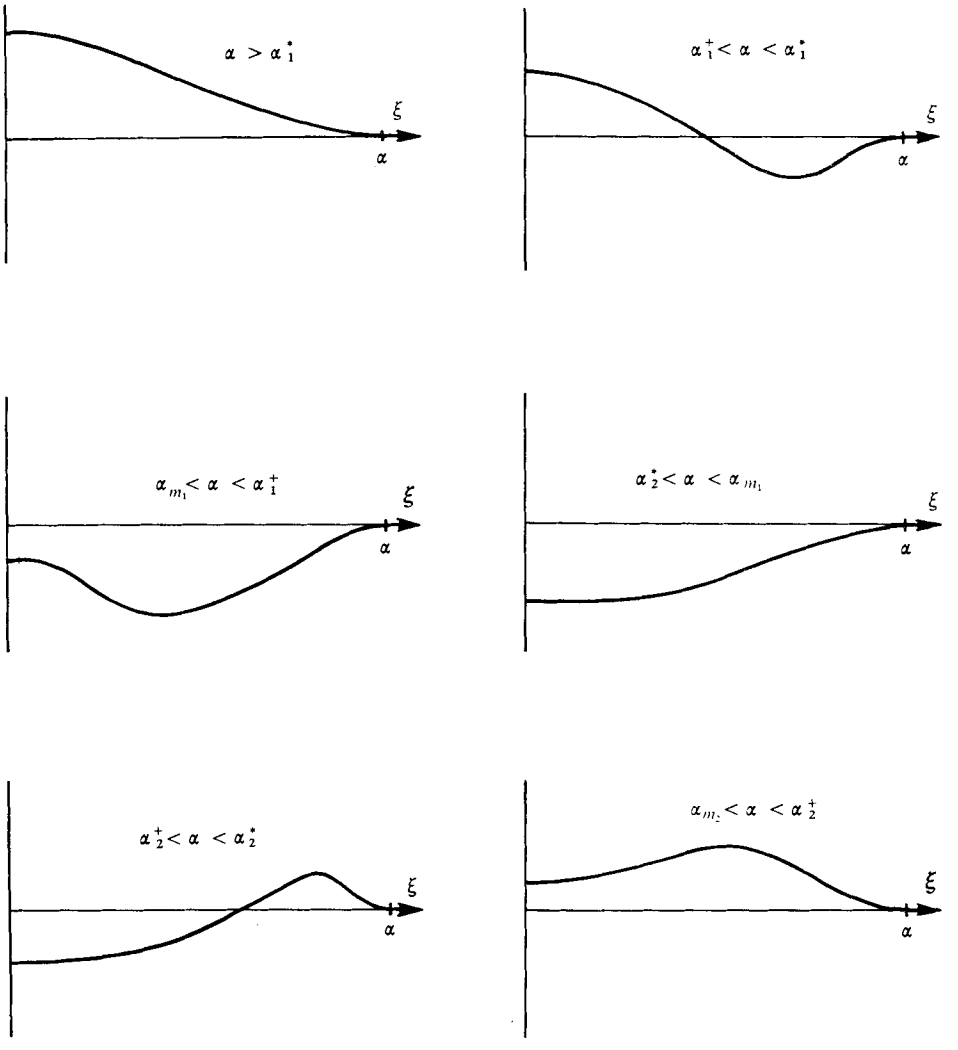

FIGURE 3. The profiles of w along the line of centres between the spheres for varying α.

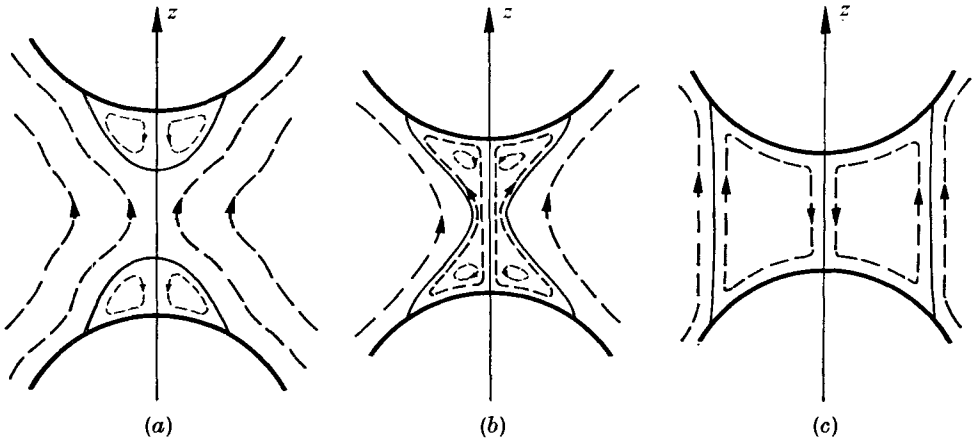

FIGURE 4. The flow structure in the primary wakes (*a*) before coalescence, (*b*) immediately after coalescence, (*c*) after coalescence when the two ring vortices have emerged.

contact. This agrees with the result proved earlier that $w(0)$ has an infinity of zeros as $\alpha \to 0$. Indeed, all the zeros of $w(0)$ are predicted to no less than four decimal places using (4.15) with only the first term retained, on account of the rapid growth of $\mathrm{Im}\,(\zeta_n)$ as n increases.

The behaviour of $w(0)$ and $w(\xi)$ for $0 < \xi < \alpha$ as $\alpha \to 0$ is consistent with the formation of wakes on the sides of the spheres which face each other. The zeros of $w(\xi)$ are at stagnation points where the wake boundaries cross the line of centres. The wakes start to form when $\alpha = \alpha_1^*$, and, as α decreases, these wakes elongate along the line of centres and touch when $\alpha = \alpha_1^\dagger$, the largest zero of $w(0)$. The two separate wakes then coalesce. Before coalescence, there is a volume of fluid trapped in each wake which rotates in a ring vortex, as illustrated in figure 4(*a*). After the wakes coalesce, these two ring vortices gradually merge into one as the distance between the spheres decreases. Figure 4(*b*) illustrates the flow pattern in the wake after coalescence but before the two ring vortices have merged. The velocity along the line of centres has maximum magnitude at two points between the origin and the spheres. Figure 4(*c*) indicates the flow pattern when the two ring vortices have merged and the maximum velocity along the line of centres now occurs at the origin. Thus the ring vortices merge when $\alpha = \alpha_{m_1}$, i.e. when $2k \approx 3{\cdot}13$. Subsequently the development of secondary wakes on the spheres commences when $\alpha = \alpha_2^*$. These wakes in turn coalesce when $\alpha = \alpha_2^\dagger$, leading to the development of tertiary wakes on the spheres, and so on. In this way, we can visualize how the infinite set of ring vortices, which characterize the flow structure when the spheres are in contact, can develop in a systematic manner if α is decreased, so that the spheres come closer together. To verify that this complex wake structure does indeed occur, it is necessary to trace out the stream surface $\psi = 0$. Without separation of the flow from the spheres, the surface $\psi = 0$ would simply consist of the spheres together with the line of centres.

The expression for ψ, as a function of general values of ξ and η, is given by (4.4) and to find the points (ξ, η) at which $\psi = 0$, other than on the spheres and the

line of centres, we found the most satisfactory approach was to fix on a particular value of ξ in the range $0 \leqslant \xi < \alpha$, having chosen α, and carry out a search over the values of η in the range $\pi > \eta > 0$ to locate the value of η at which ψ vanished. By refining the subdivisions in the η parameter so as to obtain values of ψ on either side of the zero which would be at most $\pm 10^{-9}$, the zero could then be accurately determined by interpolation. In this way we were able to obtain accurate values of the cylindrical polar co-ordinates (r, z) of the points on the surfaces $\psi = 0$, using (4.1). In fact we were able to determine r and z correct to three or four decimal places, which would give $\psi = 0$ to at least ten decimal places for each of the values of α considered.

Equation (4.4) is unsuitable for finding the points where the flow separates from the spheres, since ψ vanishes on the surface of either sphere. Furthermore, since $\partial\psi/\partial\xi = 0$ also on either sphere, to find the separation points, it is necessary to find the values of η satisfying

$$\lim_{\xi\to\alpha}\{\psi/(\xi-\alpha)^2\} = 0,$$

or, equivalently,

$$[\partial^2\psi/\partial\xi^2]_{\xi=\alpha} = 0.$$

On substituting for ψ, this equation reduces to

$$\frac{(1-\sigma^2)(\cosh^2\alpha - 3 + 2\sigma\cosh\alpha)}{8(\cosh\alpha-\sigma)^4} + (\cosh\alpha-\sigma)^{-\frac{3}{2}}\sum_{n=1}^{\infty} U_n'' V_n = 0, \qquad (4.19)$$

where $U_n'' = (n-\frac{1}{2})^2 A_n \cosh(n-\frac{1}{2})\alpha + (n+\frac{3}{2})^2 C_n \cosh(n+\frac{3}{2})\alpha$.

The value of α when separation first occurs is the largest value of α for which

$$\lim_{\sigma\to-1}\left\{\frac{1}{(1+\sigma)}\left(\frac{\partial^2\psi}{\partial\xi^2}\right)_{\xi=\alpha}\right\} = 0,$$

i.e. for which

$$\frac{(\cosh\alpha-3)}{4(\cosh\alpha+1)^3} + (\cosh\alpha+1)^{-\frac{3}{2}}\sum_{n=1}^{\infty}(-1)^{n+1}(2n+1)\,U_n'' = 0. \qquad (4.20)$$

Other solutions of (4.20) give the values of α when secondary, tertiary, etc., wakes start to form. It may be verified that (4.20) is equivalent to

$$\lim_{\xi\to\alpha}\left[\frac{w_{\sigma=-1}}{(\xi-\alpha)^2}\right] = 0,$$

showing that separation starts to occur when the second derivative of the velocity along the line of centres vanishes on either sphere. Thus the solutions of (4.20) are $\alpha = \alpha_1^*, \alpha_2^*$ and so on.

In figure 5, we have plotted the traces of the stream surfaces $\psi = 0$ in the r, z plane with $z \geqslant 0$ for $\alpha = 1{\cdot}1$, $1{\cdot}05434$, and $0{\cdot}9$. These three values of α illustrate in turn the shapes of the primary wakes when they are separate and attached to the spheres, when they are about to coalesce, and after coalescence has occurred.

Prior to coalescence, the primary wakes are similar to the inertial wake which forms on the downstream side of a sphere when the Reynolds number is increased, as shown in Van Dyke (1975). When the primary wakes make contact and

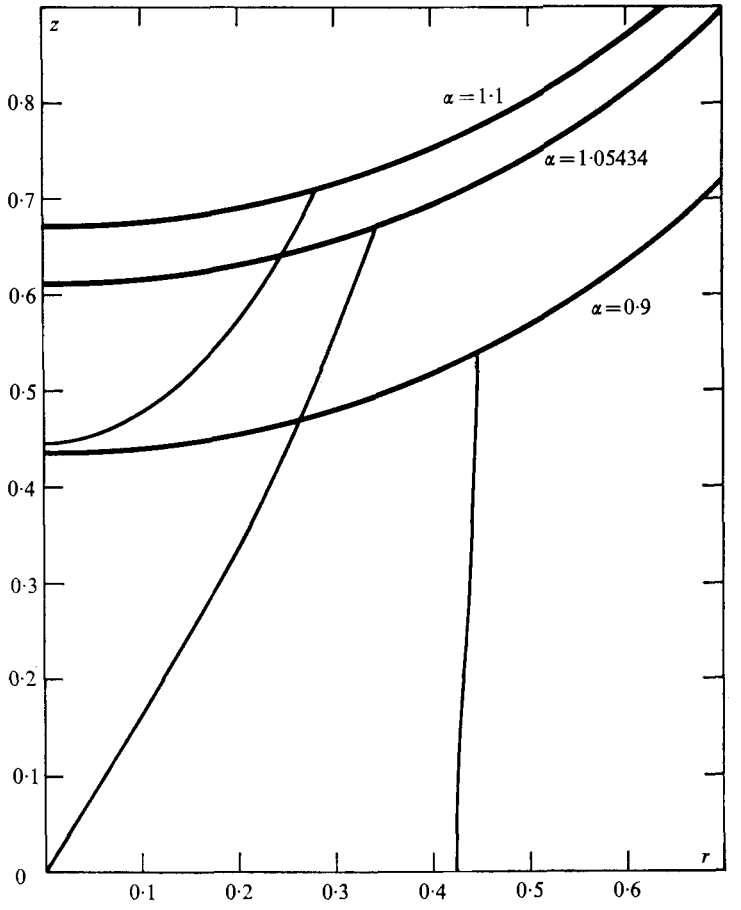

FIGURE 5. Plot of meridional sections of the stream surface $\psi = 0$ for $\alpha = 1{\cdot}1$, $1{\cdot}05434$ and $0{\cdot}9$.

coalesce, it will be seen in figure 5 that the wakes become conical in shape as this critical state is reached. This interesting feature of the flow can be verified analytically by considering the form of the stream function in the neighbourhood of the point of contact and coalescence, i.e. the origin $r = z = 0$. To carry out this examination, it is convenient to work in spherical polar co-ordinates (R, ϕ, θ), related to the cylindrical polar co-ordinates (r, θ, z) in the usual way.

Since ψ satisfies the repeated axisymmetric Stokes operator equation (2.3), and is symmetric about the plane $\phi = \frac{1}{2}\pi$, the expansion of ψ about the origin has the form:

$$\psi(R, \phi; \alpha) = A(\alpha) R^2 \sin^2\phi + B(\alpha) R^4 \sin^2\phi(1 - 5\cos^2\phi) + C(\alpha) R^4 \sin^2\phi + \ldots. \quad (4.21)$$

Since the wakes attached to the spheres coalesce when $\alpha = \alpha^\dagger$, it follows that $A(\alpha^\dagger) = 0$. Thus near the origin

$$\psi(R, \phi; \alpha^\dagger) \sim R^4 \sin^2\phi[B(\alpha^\dagger) + C(\alpha^\dagger) - 5B(\alpha^\dagger)\cos^2\phi]. \quad (4.22)$$

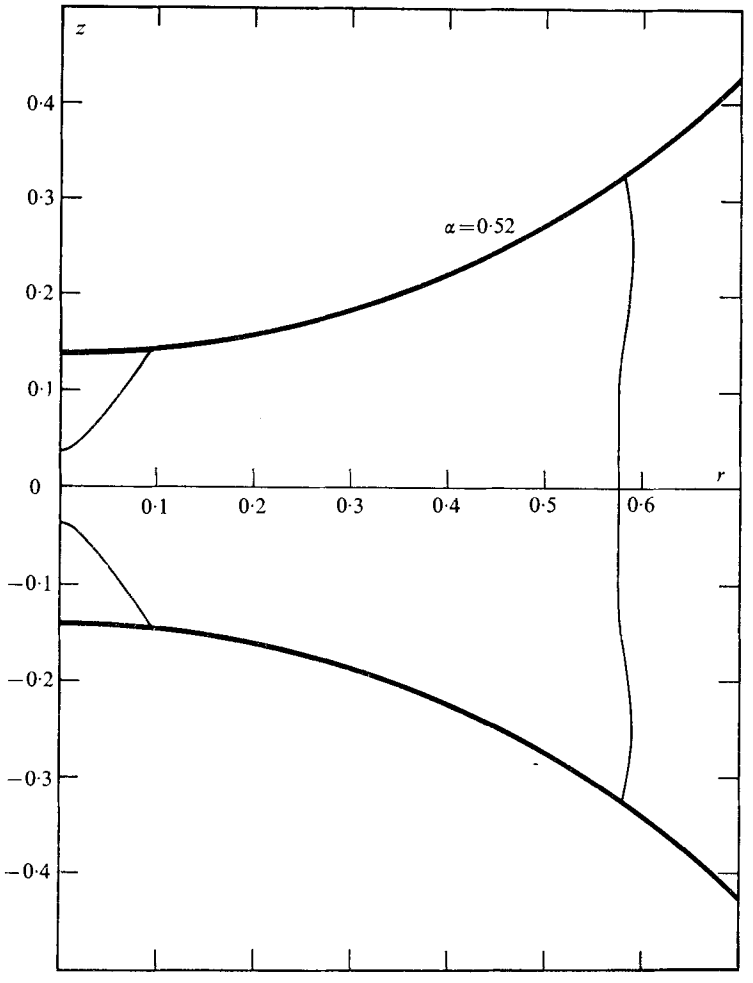

FIGURE 6. Plot of a meridional section of the stream surfaces $\psi = 0$ for $\alpha = 0{\cdot}52$.

It is therefore evident that the surface $\psi = 0$ consists locally of the axis of symmetry $\phi = 0, \pi$ together with a cone whose semi-vertical angle ϕ_c is given by

$$\cos\phi_c = \left[\frac{B(\alpha^\dagger)+C(\alpha^\dagger)}{5B(\alpha^\dagger)}\right]^{\frac{1}{2}}. \tag{4.23}$$

To determine $B(\alpha^\dagger)$ and $C(\alpha^\dagger)$ we note that the fluid velocity along the line of centres between the spheres and the radial pressure gradient at the origin are

$$w(R) = \left[\frac{-1}{R^2\sin\phi}\frac{\partial\psi}{\partial\phi}\right]_{\phi=0} = [8B(\alpha^\dagger) - 2C(\alpha^\dagger)]R^2 + \ldots, \tag{4.24}$$

$$\left[\frac{\partial p}{\partial R}\right]_{R=0} = \left[\frac{-1}{R^2\sin\phi}\frac{\partial(\Lambda^2\psi)}{\partial\phi}\right]_{R=0} = -20C(\alpha^\dagger). \tag{4.25}$$

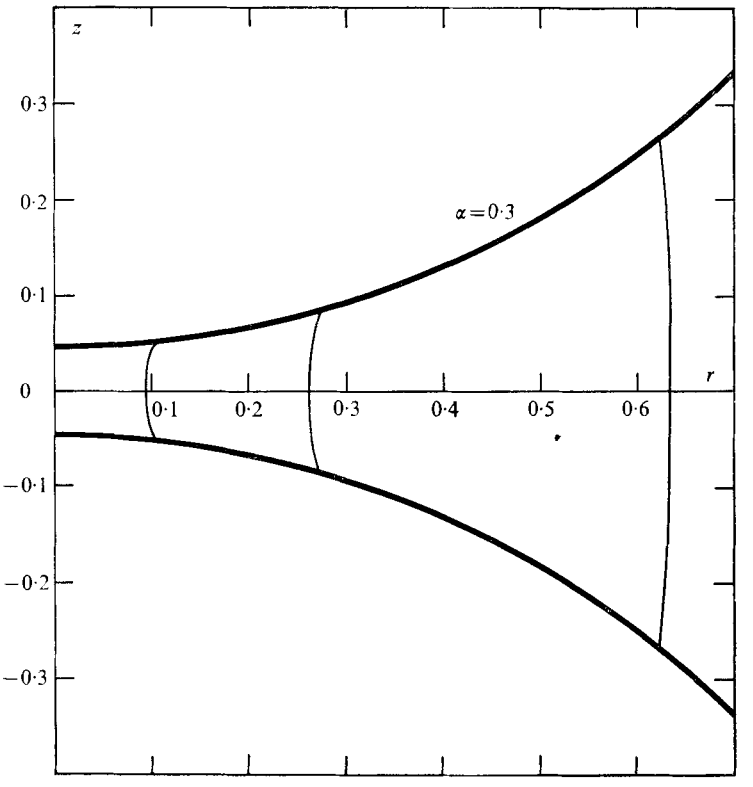

FIGURE 7. Plot of a meridional section of the stream surfaces $\psi = 0$ for $\alpha = 0{\cdot}3$.

Writing
$$F(\alpha^\dagger) = \lim_{R\to 0}\frac{w(R)}{R^2}, \quad G(\alpha^\dagger) = \left[\frac{\partial p}{\partial R}\right]_{R=0},$$
we find from (4.23)
$$\tan^2\phi_c = \frac{8F}{2F-G}. \tag{4.26}$$

We determine $F(\alpha^\dagger)$ by expanding $w(\xi)$, as given by (4.18), in powers of ξ^2 and recognizing that, to the first order,
$$\xi^2 \sim 4R^2/c^2. \tag{4.27}$$
As a result,
$$F(\alpha^\dagger) \sim -\frac{\pi}{2c^2}\operatorname{Re}\left\{(\zeta_1^2-1)\left[\frac{2(1-e^{-\zeta_1\alpha^\dagger})+\zeta_1\sinh 2\alpha^\dagger-\zeta_1^2\sinh^2\alpha^\dagger}{(\sinh 2\alpha^\dagger+2\alpha^\dagger\cosh\zeta_1\alpha^\dagger)\cos(\tfrac{1}{2}\pi\zeta_1)}\right]\right\}. \tag{4.28}$$

On the other hand, using (4.4), we find that $G(\alpha^\dagger)$ is given by
$$G(\alpha^\dagger) = \frac{2\sqrt{2}}{c^2}\sum_{n=1}^{\infty}(-1)^{n+1}(2n+1)[(4n+7)C_n-(4n-3)A_n]. \tag{4.29}$$

A function similar to $f(z)$ in (4.13) can be found which permits the following asymptotic expression for $G(\alpha^\dagger)$ to be derived:
$$G(\alpha^\dagger) \sim -\frac{2\pi}{c^2}\operatorname{Re}\left\{\frac{(\zeta_1^2-1)}{(\zeta_1^2-4)}\frac{(\zeta_1^2-5)[2(1-e^{-\zeta_1\alpha^\dagger})+\zeta_1\sinh 2\alpha^\dagger]-\zeta_1^2\sinh^2\alpha^\dagger}{(\sinh 2\alpha^\dagger+2\alpha^\dagger\cosh\zeta_1\alpha^\dagger)\cos\tfrac{1}{2}\pi\zeta_1}\right\}. \tag{4.30}$$

Combining (4.28) and (4.30) in accordance with (4.26), we can compute the angle ϕ_c for a given value of $\alpha^\dagger$. The results are contained in table 2, and suggest that ϕ_c has a limit as $\alpha^\dagger \to 0$. Now $\alpha^\dagger$ is a solution of $Q(\alpha) = 0$, where $Q(\alpha)$ is given by (4.15); hence

$$\mathrm{Re}\left\{\left(\frac{\zeta_1^2-1}{\zeta_1^2-4}\right)\frac{4\sinh^2(\frac{1}{2}\zeta_1\alpha^\dagger)+\zeta_1^2\sinh^2\alpha^\dagger}{(\sinh 2\alpha^\dagger+2\alpha^\dagger\cosh\zeta_1\alpha^\dagger)\cos\frac{1}{2}\pi\zeta_1}\right\}=0, \tag{4.31}$$

with exponentially small error introduced by retaining only the leading term. The zero ζ_1 depends on $\alpha^\dagger$ but is such that $\zeta_1\alpha^\dagger \to i\bar{\lambda}_1$ as $\alpha^\dagger \to 0$, where λ_1 is given by (3.8). Equation (4.31) may be used, as in § 3, to eliminate $\cos\frac{1}{2}\pi\zeta_1$ from the ratio F/G, thus expressing it as a ratio of imaginary parts. On substituting into (4.26) and noting that $\sin\lambda_1 + \lambda_1 = 0$, it follows that

$$\lim_{\alpha^\dagger\to 0}\tan^2\phi_c = 4 - 16\,\mathrm{Im}\,(\cos\lambda_1)/\mathrm{Im}\,(\lambda_1^2),$$

which accordingly gives $\lim_{\alpha^\dagger\to 0}\phi_c = 35{\cdot}89°$.

Figure 6 illustrates the case $\alpha = 0{\cdot}52$, when a secondary wake has formed on either sphere. The plot for $\alpha = 0{\cdot}3$, shown in figure 7, illustrates a case when primary, secondary and tertiary wakes have coalesced. The shape of the wake boundaries now takes on the appearance of that of the spheres in contact, as shown in figure 2. For all $\alpha < \alpha_1^\dagger$, there is a surface attached to both spheres which divides the main streaming flow past the spheres from a closed region in which the fluid rotates in one or more ring vortices. As $\alpha \to 0$, this stream surface becomes essentially a circular cylinder slightly pinched where it intersects the spheres.

The work described in this paper was carried out in part while one of us (M. E. O'Neill) was visiting the Department of Mathematics, University of Toronto, and was supported by the National Research Council of Canada.

REFERENCES

Abramovitz, M. & Stegun, I. A. 1965 *Handbook of Mathematical Functions*. Dover.

Bourot, J. M. 1975 *Comptes Rendus Acad. Sci. Paris*, A **281**, 178–182.

Buchwald, V. T. 1964 *Proc. Roy. Soc.* A **277**, 385–400.

Cooley, M. D. A. & O'Neill, M. E. 1969 *Proc. Camb. Phil. Soc.* **66**, 407–415.

Dean, W. R. & Montagnon, P. E. 1949 *Proc. Camb. Phil. Soc.*, **45**, 389–394.

Dorrepaal, J. M., Majumdar, S. R., O'Neill, M. E. & Ranger, K. B. 1976*a* *Quart. J. Mech. Appl. Math.* (in press).

Dorrepaal, J. M., O'Neill, M. E. & Ranger, K. B. 1976*b* *J. Fluid Mech.* **75**, 273–286.

Finn, R. & Noll, W. 1957 *Arch. Rat. Mech. Anal.* **1**, 97–106.

Gradshteyn, I. S. & Ryzhik, I. M. 1965 *Tables of Integrals, Series and Products*. Academic.

Jeffery, G. B. 1922 *Proc. Roy. Soc.* A **101**, 169–174.

Moffatt, H. K. 1964 *J. Fluid Mech.* **18**, 1–18.

Schubert, G. 1967 *J. Fluid Mech.* **27**, 647–656.

Stimson, M. & Jeffery, G. B. 1926 *Proc. Roy. Soc.* A **111**, 110.

Van Dyke, M. 1975 *Perturbation Methods in Fluid Mechanics*. Stanford: Parabolic Press.

Wakiya, S. 1975 *J. Phys. Soc. Japan*, **39**, 1113.

Wannier, G. H. 1950 *Quart. Appl. Math.* **8**, 7–22.